ECO2 project number: 265847

Deliverable Number D3.1: Technical synthesis report;
WP3; lead beneficiary number 5 (UiB)

TECHNICAL SYNTHESIS REPORT ON DROPLET/BUBBLE DYNAMICS, PLUME DYNAMICS AND MODELLING PARAMETERS, USE OF HYDRO-ACOUSTICS TO QUANTIFY DROPLET/BUBBLE FLUXES, AND CARBONATE SYSTEM VARIABLE ASSESSMENT

Guttorm Alendal, Abdirahman Omar, Alden R. Denny, Tamara Baumberger, Stan E. Beaubien, Lisa Vieldstädte, Marius Dewar, Baixin Chen, Rolf B. Pedersen, Cinzia De Vittor, Truls Johannessen.

1. Executive Summary

This report summarises the cruise activities in ECO2-WP3 related to understanding processes during CO_2 seeping to the marine environment. Three main themes are covered; bubble plume dynamics and CO_2 transport, the use of hydro-acoustic as a tool to detect, localize and quantify CO_2 seeps, and the marine carbonate system.

The huge amount of data collected during the field campaigns is still not fully interpreted, and analysis will continue and further results will be published in the immediate future. However this summary report symbolises a change of pace in WP3; the focus changes from data gathering toward the numerical scenarios to be performed in the central North Sea. Further publications from synthesising cruise data will continue in parallel.

During the field campaigns characteristics of single bubbles, i.e. size, shape, dissolution rates and rise velocity, has been studied at the different natural seep locations. In addition Geomar performed a release experiment in the North Sea. These studies have, and will continue to improve important process models used within the model framework that will be used to predict the fate of seeped CO_2 in the sea. Details on model calibration and validation will be treated in more detail in D3.3.

Further, near-field plume hydrodynamics at seepage sites have been investigated to determine the plume boundary conditions, and the evolution of dissolved and physical constituents. Fieldwork at Panarea, with high CO_2 emissions, shows significant tidal control on dissolved CO_2 movements and mixing. The natural bubble size spectrum is broad with largest bubbles having radius larger than 5 mm allowing gas transport to shallower depths. Moreover, the fluorescence tracer experiment established an additional upward transport component caused by rising gas bubbles as well as by advective hydrothermal fluids. Both fluorescence data and pCO_2 data show that these mechanisms are effective as long as the bubble number density is high enough to entrain enough surrounding water and/or a

significant density-difference between warm hydrothermal fluids and the surrounding water remains.

For a North Sea case scenario, where water depth are ~ 100 m and no thermal effects is present, this suggests that the impact of CO_2 seepage is limited to bottom waters. The dilution of the dissolved CO_2 is also higher in a high and variable current environment as in the North Sea. Dissolution of CO_2 from small bubbles is particularly rapid, indicating that the environmental impact on the marine benthos is highest from this size distribution.

This is supported by the Geomar gas point release experiment in the North Sea; the impact of leakage at a rate comparable to the experiment (~130 kg/day) is limited to bottom waters (1-5 m above ground) and a small area around the gas source (50 m). Tidal cycles and strong currents, which are a prominent feature for the North Sea, will efficiently dilute the solute, and significantly diminish the footprint in the far field. This indicates that the environmental impact from a point source will be very localized, with limited consequences for the marine environment. However, the limited extent of the signal makes detection and localization of a leak a bigger challenge. How the impact will be for diffused leaks, i.e. a number of spatially distributed, but interacting, leakage points, remains to be studied.

Acoustic methods to detect bubble plumes and to quantify fluxes of bubbles into the water column have been performed. From the Jan Mayen vent fields and Panarea site it is clear that multibeam echo sounders (MBES) is a powerful tool for determining the occurrence and dynamics of bubble plumes in the water column. Given the dramatically improved survey swath provided by MBES over single-beam echo sounders (SBES), the MBES is much more efficient in surveying for seafloor gas seeps. In addition to locating the seeps the concurrent acquisition of bathymetric soundings provides a detailed look at the seafloor features that may be related to the gas seeps. SBES systems are appropriate for examining time-series on a single location, and could be used to calculate the rise velocity of bubbles from a single source, but given the narrow water column region surveyed by the single beam these systems are not appropriate for locating gas seeps on the seafloor.

While MBES systems are powerful tools for locating seafloor gas seeps, they work best on dedicated water column surveys and are highly susceptible to interference from other acoustic systems. MBES surveys run concurrent with SBES systems must be set up with timing offsets to prevent signal interaction. As well, it is not possible to run MBES and sub-bottom profiling parametric systems concurrently. With these stipulations, multibeam sonar systems have the potential to provide the highest resolution, fastest, and consequently least expensive method for monitoring for potential gas seeps possible with current technologies.

The few available results so far indicate that measurements of the carbonate system in the water column are suitable for quantification of the effects of seepage on the water chemistry. High carbon concentrations have been reported for natural CO2 seepage sites whereas above the industrial subsea CO2 storage Sleipner only normal background values have been observed.

2. Introduction and background

Although a well-chosen and well-engineered sub-seafloor CO_2 storage site is not expected to leak, we must have a clear understanding of the behaviour of CO_2 in the marine environment to ensure that we are prepared for any eventuality, no matter how unlikely it may be. This is the rationale behind the *EC directive (2009/31/EC)* on geological storage of CO_2, as well as recommendations from *OSPAR* and *London Conventions*. Fulfilment of Article 13 of the EC directive (monitoring) requires the establishment of a framework for future "*detection of leakage*" and "*detection of significant adverse effects for the surrounding environment, human health, or users of the surrounding biosphere*".

As part of any CO_2 storage projects government and international regulations will therefore require risk and environmental status assessments in order to sustain future monitoring programs, as well as describe protocols for leakage detection and remediation efforts. In the case of sub-seabed storage in geological formations these assessments will have to include potential impact on the marine environment and the seafloor, and will have

to outline a subsequent monitoring program for detection, localisation and quantification of a leak.

In this respect it is important to understand the fate of CO_2 seeping into the overlying water column, which is the aim of WP3. Only with a proper understanding of the processes involved during a seep will an estimate of the spatial and temporal footprint of a potential leak be reliable. Such a footprint is essential for subsequent impact assessments and for designing a monitoring program for the marine environment.

During a hypothetical leak scenario CO_2 gas bubbles/droplets will ascend through the water column and gradually dissolve, acidifying the entrained water. When simulating such a bubble /droplet train or plume the two most important sub-models are considered to be how fast the bubbles/droplets rise, and how quickly they dissolve. In addition local conditions will determine how quickly the elevated concentration of CO_2 will be diluted, hence local turbulent mixing and transport, and understanding of the carbonate system is an integrated part of a site survey. Further, the acoustic fingerprint of CO_2 bubbles is important for further assessment of detecting seeps through hydro acoustics.

Although laboratory experiments and modelling can, and has been, performed, ECO2 turns to natural analogues for a more complete (and realistic) understanding of a possible seabed leak of CO_2. This is particularly important because CO_2 leakage presents some unique challenges. First, it is highly soluble and thus CO_2 bubbles will dissolve extremely rapidly; this makes bubble detection more challenging using hydro-acoustic techniques. Second, dissolved CO_2 increases the density of seawater, and thus high CO_2 concentration seepage will likely remain close to the seafloor.

With focus on the extensive ECO2 cruise program this report aims to give an overview of present understanding and achievements made within the following topics:

- *Bubble and plume dynamics and modelling parameters.*
- *Use of hydro-acoustics to detect a seep.*
- *The carbonate system*.

There are still data sets from cruises that remain to be analysed in the context of these topics, and this work continues and will be reported through publications accordingly. However, the main focus for the remaining ECO2 period will be on carrying out the scenarios, in collaboration with the other work packages.

Since the cruises have, to varying degrees, carried out work within all the three topics, a summary of the most relevant cruises will be given. After which the three topics will be treated separately.

3. The Cruise program

ECO2 has had an extensive cruise program; the cruises with most relevance to the three topics treated here are listed in Tab 1. Most of these cruises have received national funding from respective countries, but results are reported within the ECO2 framework. For this report three sites are of special interest, the Sleipner area, the Jan Mayen Vent Field (JMVF) and the Panarea site.

Since the WP3 modelling scenarios will be conducted in the Sleipner area, the cruises to the central North Sea have provided valuable environmental data, including carbonate system data, in addition to the historical data already collected. In addition, due to the natural CH_4 seeps in the area, these cruises also provide valuable demonstration of hydro-acoustics as a detection and quantification tool, as discussed later in this report. The use of hydro-acoustics is further demonstrated for CO_2 at JMVF.

Cruises conducted with relevance to the deliverable			
Study site	**Date**	**Research vessel**	**Lead institute**
Sleipner and Salt Dome Juist	29/05 - 14/06/2011	RV Alkor (AL 374)	GEOMAR
Panarea	28/05 - 13/06/2011	Small Boat (ECO2-2)	MPI
Jan Mayen vent field	10 - 23/06/2011	G.O. Sars (CGB- ECO2 -2011)	UiB
Sleipner	24/06 - 02/07/2011	G.O. Sars (CGB- ECO2-2011B)	UiB
Panarea	27/07 - 01/08/2011	RV Urania (PaCO2)	GEOMAR
Salt Dome Juist and Sleipner	16 - 24/04/2012	RV Heincke (HE- 377)	MPI
Panarea	02 - 21/06/2012	Small Boat (ECO2-3)	MPI
Panarea	05 - 10/06/2012	Small Boat (ECO2-4)	UniRoma1 / OGS
Sleipner	22 - 30/06/2012	G.O. Sars (CGB- ECO2-2012A)	UiB
Jan Mayen vent field	23/07 - 03/08/2012	G.O. Sars (CGB- ECO2-2012B)	UiB
Sleipner	20/07 - 06/08/2012	RV Celtic Explorer (CE12010)	GEOMAR
Panarea	20 - 24/08/2012	Small Boat (ECO2-5)	UniRoma1 / OGS
Sleipner	02 - 28/09/2012	RRS James Cook (JC077)	NOC
Panarea	19 - 31/10/2012	Small Boat (ECO2-6)	UniRoma1 / OGS
Eckernfšrder Bay	04 - 11/11/2012	RV Alkor (AL 404)	GEOMAR
Sleipner and Blow- out site	22/03 - 08/04/2013	RV Alkor (AL 412)	GEOMAR
Panarea	21-31/05/2013	Small boats (ECO2-7)	UniRoma1/OGS

Figure 1: List of relevant cruises within ECO2.

The natural CO_2 seeps have been used as natural laboratories to increase our level of understating of processes involved and confine important input parameters for modelling and prediction. Especially the Panarea area has been shown to be of great value due to its accessibility.

Only brief descriptions of some of the cruises focusing on Panarea, the North Sea, and to the Norwegian Sea, are given here. For a more details please refer to the individual cruise reports.

3.1. Panarea

The **Panarea natural** CO_2-release field is part of the Aeolian Archipelago and submarine gas seepage is common around the volcanic island *(Aliani et al. 2010; Caramanna and Voltattorni 2011)* The gases are emitted at shallow water depth and have a high CO_2 content (>95%). Active seepage has been reported since ancient times and occurs at a wide range of gas flows from diffuse bubble ebullition with large footprints to isolated bubble plumes or even single bubble chains; this variability allows for the study of a broad range of

seepage modes. Hence, Panarea constitutes an ideal natural laboratory for investigating the impact of potential CO_2 leakage on the marine environment.

UniRoma1 and **OGS** have conducted a total of 5 field campaigns to the Panarea site (July 2011, June 2012, August 2012, October 2012, and May 2013), with work for WP3 being performed during each campaign. Discrete samples collected from the deep water column during the July 2011 campaign on the R/V Urania (a EuroFleets cruise linked to ECO2), from benthic chambers, and from shallow water profiling from small rented boats within the main seep areas were analysed for a full suite of components of the carbonate system. These results, in addition to being used to interpret chemical and biochemical dynamics in the sampled environments, were also used to compare measured values with those calculated using the carbonate equilibrium program CO2Calc. Bubble dynamic experiments were conducted using a 3 m tall support structure, with measurements of bubble rise velocity, bubble size, bubble gas composition and water column chemistry measurements being conducted to collect data for input into the Discrete Bubble Model (DBM) of McGinnis et al. (2011). To study response time and parameter comparison, the UniRoma1-developed GasPro-pCO_2 probe was tested against the commercially available Contros HydroC sensor, and the GasPro-pCO2 probe response was compared with that of a CTD-mounted pH meter. Finally a total of 20 GasPro-pCO_2 probes were deployed along a profile in the water column for a 2.5 day period to monitor fate and transport of the dissolved CO_2 originating from the natural CO_2 leaks. The low cost of these probes allows for such mass deployments which helps better characterise dynamic mixing processes in the water column for eventual hydrodynamic modelling.

Geomar conducted investigations at Panarea in June 2012 and 2013 that encompassed geochemical analyses (pCO_2, TA, DIC, B, H_2S), hydro-physics (conductivity, temperature, pressure) as well as local hydrodynamics (current flow) aimed at understanding bubble dissolution and solute dispersion processes. The second campaign in 2013 particularly aimed at filling parameterization gaps of the previous cruise (i.e. bubble rise velocity, and shrinkage rate). A bubble parameterization rack (BPR) enabled the

measurement of bubble sizes and rise velocities optically, at high resolution, from the seafloor to 80 cm above the seabed. Water and gas samples were taken at various depths and locations to analyse changes in gas bubble composition, solute gas concentrations (i.e. CO_2, O_2, N_2, H_2S) and total alkalinity in ambient seawater as a function of bubble raise height. Additionally, a fluorescence tracer experiment was performed to visualize plume dynamics and solute dispersion in that area for the first time. Chemistry analysis, as well as HD-image and video analysis are in process and will enable us to test and improve parameterizations used to model bubble dissolution. Parameterizations for gas bubble plumes (i.e. entrainment of water) will be implemented and tested using the fluorescence data.

Stationary measurements of pCO_2 and local current flow provide information on solute dispersion over a time period of 7 days. In combination with entire gas flux measurements the data set is being used to test the applicability of the plume model to quantify leakage rates.

3.2. The North Sea and the Norwegian Sea

University of Bergen (UiB) has visited both, the **Jan Mayen vent fields (JMVF)** (Expeditions CGB-ECO2-2011 and CGB-ECO2-2012B) and the **Sleipner area** (Expeditions CGB-ECO2-2011B and CGB-ECO2-2012A), twice by R/V G.O. Sars. The water column of both target areas was investigated by using a CTD/rosette package and subsequent analysis of the according water samples. The CTD was equipped with the standard CTD sensors as well as with auxiliary sensors for dissolved oxygen and Eh (redox potential; JMVF only). Spatial profiling of the water column provides information about its physical properties. The analysis of sensor data and water samples collected at selected places within the water column provides information about the according chemical composition. UiB investigated the water column was by using acoustic (echo sounder) and visual (ROV HD-camera) methods. In addition, measurements of dissolved gases, such as CH_4, O_2 and H_2 were conducted, as well as for pH and alkalinity and the water column was sampled for shore-based analysis of anions, cations and nutrients.

At the *Jan Mayen vent fields (JMVF)* the water column profiles concentrated on focused high-temperature vents and on areas with diffusive fluid flow, both characterized by high CO_2 volatile contents. Analysis of samples collected above the high CO_2 systems at the JMVF will provide information on potential biogeochemical tracers of CO_2 seepage within the chemical plume. Additional water column samples were collected within the bubble plume at the JMVF by the uprising ROV. These samples will provide information on the difference in the bubble and chemical plume regarding the chemical composition. In addition, visual and hydro-acoustic investigations of bubbles rising in the water column at both Sleipner (CH_4) and the JMVF (CO_2) were performed. A 15 minutes record of single bubbles rising from the JMVF (site Trollveggen) up through the water column was achieved. This comprehensive data set will be analysed within the next few months regarding different rising speeds and bubble dynamics.

In the Sleipner area **GEOMAR** conducted a CO_2 release experiment, at the seabed and collected video data of initial bubble sizes as well as geochemical data of the dispersion of dissolved CO_2 downstream of the release spot. Additionally, data of the local current regime were measured with an ADCP over a few tidal cycles. This experiment is described further in The Gas release experiment

In the autumn of 2012 the **National Oceanography Centre** conducted a research programme at the *Sleipner area* (Cruise JC077). This cruise was intended mainly to demonstrate the use of AUV technology (the Autosub) for the survey of large areas of seafloor for indications of seepage. The AUV was equipped with a number of sensors (pCO_2, pH, Eh, Chirp) that may be used as indicators of leakage. The AUV successfully detected bubble leakage over the Hugin fracture area and a number of abandoned wells in the CNS. The cruise demonstrated that AUV technology in combination with a focussed sampling strategy (water column, video work and coring) could be used as a means of performing high resolution, wide area surveys over existing and proposed CCS location.

4. Part I: Bubble/droplet plumes

4.1. Introduction and rationale

Gaseous or liquid CO_2 seeps from the seafloor represent a multiphase and multicomponent flow. CO_2 will be less dense that seawater shallower than approximately 3000 meters. In addition the onset of hydrates may be seen in Figure 2, along with the gaseous or liquid phase of the CO_2.

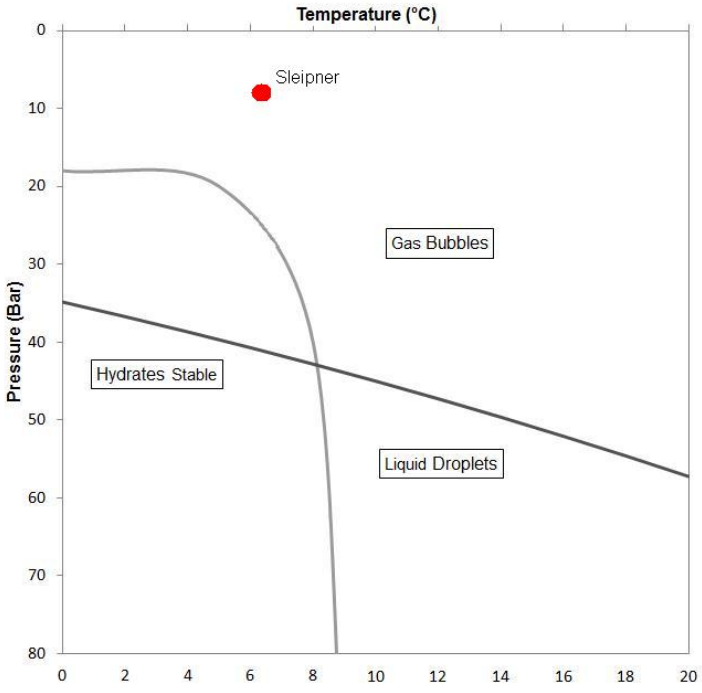

Figure 2: Phase diagram for CO2. Sleipner pressure and temperature are indicated by the red dot.

Depending on temperature, the border between gaseous bubbles and liquid droplets is at approx. 500 m. Hence, CO_2 reaching the seafloor will create bubbles/droplets ascending through the water column. Since the modelling scenarios to be performed will be

at Sleipner we will refer to the dispersed phase as bubbles. Most of the discussion can be transferred to droplets.

Depending on the flux rate, a seep location may create individual bubbles, a bubble train or a plume (Figure 3). Due to Newton's actio-reactio law; the retarding friction force felt by the individual bubbles will be felt as a lifting force by the adjacent water masses. If the number of bubbles is large enough, a two phase, two-component, bubble plume will be generated. The lifted (entrained) seawater will be brought vertically and, in case of stratification, into less dense environment.

Figure 3: Illustration of different flow regimes (UniRoma1 – OGS).

Simultaneously the CO_2 in the bubbles will be dissolved into the adjacent water parcels, slightly influencing the seawater density. Even though the influence from a single droplet is too small to impose any dynamical change, if there is enough bubbles present the influence may be significant. Within and in the vicinity of the bubble plume the increased CO_2 concentration will lead to increased seawater density, creating a water package with negative buoyancy. Hence two major competing driving forces, 1.) lift from ascending bubbles and 2.) sinking tendencies due to increased density, are present in such a bubble plume.

The increased CO_2 concentration will also lead to an acidification of the seawater, with possible environmental impact *(Blackford et al. 2010).* Once the acidified water is separated from the influence of the bubble stream, if the density contrast is significant enough it will descend to deeper waters (*Alendal et al., 2001, Dewar et al. 2013;*). As it descends the concentration will be diluted due to diffusion and local turbulent mixing, until reaching the seafloor or level of neutral buoyancy, which ever occur first. The spatial extent

of the environmental footprint is hence highly dependent on the local current and mixing regime.

On larger scales, local and regional currents might bring portions of the CO_2 to the surface, with rapid outgassing as a possible consequence, or into deeper waters. In the latter case the ocean might serve as a buffer for the atmosphere *(Drange et al., 2001)*.

A full description of a seep will have to include a number of scales, from internal flow within each individual bubble, how mass is transferred across the boundary and motion of the bubble due to buoyancy and local currents. The simulation of large volume flux rates, i.e. large amounts of individual bubbles, is a tremendous task and in all practicality impossible. The required computational resources would be too high. Even more resources would be required if an ensemble of realisations is needed to build probability distributions and most likely impacts from a leak.

The governing equations for a two-component, two-phase, fluid will be conservation equations for mass, momentum and energy for each of the component. As a first assumption it is assumed that the bubble content has the same temperature as the surrounding, and that internal energy changes due to chemical processes can be neglected. These assumptions simplify the thermodynamic considerably, it is reduced to an Equation of State (EOS), and the energy equation for the dispersed phase is fulfilled automatically.

The two remaining equations for the bubbles, the mass and momentum equations can be described either in Lagrangian or Eulerian coordinates. In the former individual bubbles is followed, which is practical only for a small amount of bubbles. In the field description, Eulerian, the volume fraction occupied by the bubbles within a control volume is modelled (*Alendal & Drange, 2001; Sato & Sato, 2002; Chen et al., 2003)*. This is the approach used in both the plume models used within ECO2.

In either of these descriptions the mass and momentum coupling is taken care of through a mass transfer sub-model, and through interfacial friction. Often the momentum equation is simplified further by assuming that the bubbles follow the local currents in

addition to experience a vertical terminal velocity. This vertical velocity is modelled by balancing buoyancy and interfacial friction.

Due to this the two most important processes, mass transfer and interfacial friction, with emphasis on the models used by the ECO2 partners, will be described. A full documentation of the individual models, and further details on parameters used, is given in another ECO2 deliverable, D3.3 Numerical Models.

4.2. The Characteristics of multicomponent seeps.

4.2.1. Ascending single bubbles; characteristic numbers and modelling.

A single bubble ascending in a fluid is by nature a complex hydrodynamical problem, involving moving boundaries between two different fluids possible in different phase. *(Clift, et al., 1978; Brennen 1995)*.

Following the arguments of *Smolianski, et al. (2008)* the problem of a gas bubble ascending due to buoyancy is characterised by eight independent dimensional quantities; the densities, viscosities, gravity, surface tension, space and time. And, according to the Buckinghams Π theorem, five independent non-dimensional groups might be formed. These are usually chosen to be the density ratio ρ_1 / ρ_2, the viscosity ratio μ_1 / μ_2, a non-dimensional time $T = t\mu_1 / \rho_1 d_e^2$ in addition to two of the following non-dimensional numbers,

$$M = \frac{g\mu_1^4}{\rho_1 \sigma}, \quad Eo = \frac{g d_e^2 \rho_1}{\sigma} \quad \mathrm{Re} = \frac{\rho_1 d_e U}{\mu_1} \quad ,$$

respectively, the Morton, Eotvos and Reynolds-number. Here the characteristic length

$$d_e = \left(\frac{6V}{\pi} \right)^{1/3}$$

is the volume-equivalent diameter of a bubble of volume *V*, and *U* is a characteristic rise velocity of the bubble. Another number frequently in use, replacing the Eotvos number, is the Weber number

$$We = \frac{\rho_l U^2 d_e}{\sigma}.$$

The Morton and the Eotvos numbers are given *a priori* for given fluids, while to evaluate the Reynolds and the Weber numbers require a characteristic velocity to be defined, hence can only be estimated after measuring the velocity.

Ascending bubbles will always be an unsteady process, involving wobbling, interfacial waves and disturbances, and change in bubble shape. Based on the non-dimensional numbers, and a number of experiments, it is possible to define different shape regimes *(Clift et al., 1978).* Small bubbles will be spherical, and the equivalent diameter is the diameter of the bubble. As the bubble size increases the outer flow past the bubble will separate, creating a wake behind the bubble. Due to the difference in pressure at the surface, the droplet will change shape, to become more elliptical, through the spherical cap regime, until the largest bubbles that form skirts behind the bubble.

Impurities on the surface, and hydrate formation at low temperatures (below 4-8°C and deeper than 180-400 meters (*Bigalke et al., 2008; Bigalke et al. 2010)* can affect the dynamics and reduce the dissolution rate (*Aya et al.,* 1997; *Mori and Mochizuki,* 1998; *McGinnis et al., 2006*). The variation of the dynamics may be taken into account within the drag coefficient (*Bigalke et al., 2008; Bigalke et al. 2010)* seen in Sec 4.2.2, where the value varies with shape and size. In the correlation by *Bigalke et al.* [2008; 2010] the drag coefficient varies depending on the bubble size, shape through Morton, Eotvos and Reynolds-numbers, but also the hydrate formation or impurity quantities are taken into account through the surface tension.

The variation in dissolution rates may be taken into account through the solubility. However *McGinnis et al.* [2006] show through experimental results from *Bigalke et al. (2008;*

2010) that smaller methane bubbles (<3.5mm diameter), especially those near the hydrate stability field, not only form hydrates within the bubble structure but also form a complete gas hydrate rim. This greatly reduces the dissolution rate and is a sudden change in dissolution rate from bubbles with the presence of hydrates at larger sizes. This can be considered as a frozen bubble, and is modelled through a modification to the mass transfer coefficient from *Zheng and Yapa, (2002)* by an increase in the diffusivity exponent (*McGinnis et al.,* 2006) as shown in Sec. 4.2.3 for clean versus dirty bubbles.

4.2.2. The slip velocity

When simulating single droplets seeping to the ocean, the internal and external flow at individual droplets are not resolved. It is considered adequate to assume that the relaxation time of the bubbles will be much shorter that the characteristic timescale of changes in the carrier phase, in this context the seawater. It is assumed that the bubbles adjust to the local current, and an additional vertical velocity, often denoted the terminal or slip velocity, is modelled through a balance between the buoyancy felt by the bubble, and friction felt at the interface. Hence

$$U_T = \sqrt{\frac{8gr(\rho_c - \rho_d)}{3C_d\rho_c}}$$

Shape and form influence friction, which is again dependent on the relative velocity. This leads to a further splitting of the friction factor C_D

$$C_D = f_c D$$

in which f_c is a friction factor, while D is a deformation factor. Both of these are assumed dependent on the non-dimensional numbers defined above. Especially the friction factor is assumed to be dependent on the Reynolds number, and hence on the slip velocity.

With the exception of a few in-situ experiments by MBARI *(Brewer et al. 2002; Gangstø et al., 2005)* and some laboratory experiments (*Bigalke et al. 2008; 2010)* the parameter estimation have had to rely on more general models utilizing a number of

experiments using different gases, see for instance *Bozzano and Dente (2001; 2009*). The data from *Bigalke et al. (2010*) has been used to estimate parameters. The sensitivities and uncertainties in the parameter estimations have been addressed in *(Hvidevold et al. 2012; 2013*).

A more heuristic model, based on experimental data, as presented by *(Wüest et al., 1992):*

$$U_T = \begin{cases} 4474 r^{1.357} & r < 0.69mm \\ 0.23 & 0.69mm < r < 4.9mm \\ 4.202 r^{0.547} & r \geq 4.6mm \end{cases}$$

is being used in the *Geomar model.* This model shows consistency with observations of the Geomar gas release experiment, where single gas bubbles rose in the absence of bubble plume dynamics. However, natural rising gas bubbles (Panarea) exceeded modelled rise velocities, which were significantly faster. Optical data are currently evaluated and correlated to seepage activity (gas flux and seep footprint) to develop additional parameterization of entrained water velocity that is needed as a critical gas flux is exceeded.

4.2.3. The mass transfer;

In a similar fashion as for the slip velocity it is assumed that the mass-transfer can be modelled without having to resolve the small-scale processes. A Ficks like law is introduced

$$\frac{d}{dt} M_d = -A_d K M_{CO_2} \left(C_s - C_\infty \right)$$

in which the change of mass inside the bubble M_d with respect to time is proportional to the surface area of the bubble, A_d, and the gradient in concentration between saturated concentration at the bubble interface and the ambient $(C_s - C_\infty)$. A mass-transfer coefficient, $K = K(\mathrm{Re})$, with unit as velocity, is assumed dependent on the locale shear velocity and turbulent mixing, as indicated by the Reynolds number dependency. Hence the mass transfer is coupled with the slip velocity. M_{CO_2} is the molecular mass of CO_2.

Often the mass-transfer coefficient is linked to the Sherwood number

$$Sh = \frac{Kd_{eq}}{D_i}$$

which is the ratio of convective versus diffusive mass transfer and may also be used in the above equation to calculate the dissolution rate. It is common to use either the mass-transfer coefficient or the Sherwood number to define correlations, depending on whether they are bubbles (mass-transfer coefficient) or droplets (Sherwood number).

Similar to the rise velocity, the mass transfer coefficient, K, of gas bubbles in seawater dependents on the size, shape and cleanliness of bubbles as well as the specific gas diffusivity in seawater. For spherical and ellipsoidal bubbles, the turbulent flow at the bubble interface, which is induced by the buoyancy momentum, enhances mass transportation from the bubble to seawater (*Chen et al., 2009*). This is because the thickness of the diffusive boundary layer at the bubble interface is reduced with increasing rise velocity and turbulences (*Leifer et al., 2002*). For greater bubble sizes the mass transfer rate reduces as the bubble tends to a spherical-cap shape.

Sets of empirical mass transfer correlations, both for clean and dirty bubbles, have been suggested *(Leifer et al., 2000; Zheng and Yapa, 2002*; *McGinnis et al., 2006*). *Zheng and Yapa (2002)* proposed the following empirical equations, as a combination of the equations originally developed by *Johnson et al. (1969)* and *Clift et al. (1978),*

$$K = \begin{cases} 0.0113\left(\dfrac{U_T D_i}{0.45+0.4r_e}\right)^n & r_e < 2.5mm & \text{spherical} \\ 0.065 D_i^n & 2.5mm < r_e < 6.5mm & \text{ellipsoidal} \\ 0.0694\left(2r^{0.25} D_i\right) & r_e > 6.5mm & \text{spherical cap} \end{cases}$$

The above equations give the mass transfer coefficient [m/s] for various bubble shapes and sizes, where the equivalent bubble radius is given in [cm], and the molecular diffusion coefficient of the considered gas in water, Di, is given in [cm/s^2]. The exponent, n, has been determined as 0.5 and 0.67 to calculate mass transfer velocities for clean and dirty bubbles, respectively. *Zheng and Yapa (2002)* tested this set of equations using CO_2 bubbles in fresh water and in 90.6 aqueous glycerol solution, respectively, under atmospheric pressure and room temperature. Even though the model predicts experimental data very well, it should be noted that the pressure effects at water depths ≥100 m (≥ 1 MPa) have not been studied experimentally and are not yet fully understood from a theoretical perspective (*Chen et al., 2009*). Geomar currently tests the empirical equations of mass transfer by correlation to geochemical and optical derived field data (Panarea 2013). This provides new insights on CO_2 bubble shrinkage rates and will be used to test and optimize mass transfer ECO2 activities and results.

4.3. ECO2 field activities

4.3.1. Panarea activities

There are two parallel bubble dynamic experiments being conducted at the Panarea site, one conducted by UniRoma1 / OGS and the other by GEOMAR. Although conducted in the same location, the various differences (experimental setups and modelling, researchers, time periods with different water column conditions, etc.) will allow for a final comparison and sensitivity analysis that should help define the precision of the results as well as the most influential parameters. The experimental setup and results obtained thus for the two experiments are summarised below.

The UniRoma1 / OGS experiments were conducted primarily during a campaign in October 2012, based on tests and experience gained during previous visits to the site. The experiments were conducted using a light-weight, robust, 3 m tall, 1 x 1 m square structure made of tubular iron rods that had a 10m tall guide mounted on the front face for an HD video camera deployment and a dark blue cloth mounted on the back face (10 m tall) for contrast and distance from bottom measurements. The structure was deployed at a depth of

about 12 m in a pockmark in which natural CO_2 leakage is occurring. Bubbles were made using this gas, but with a system which allowed for control of both bubble size and bubble numbers. The use of the *in situ* gas, within a leakage area that impacts on the surrounding water column, allowed us to conduct the experiment in real-world leakage scenario but with control on bubble characteristics.

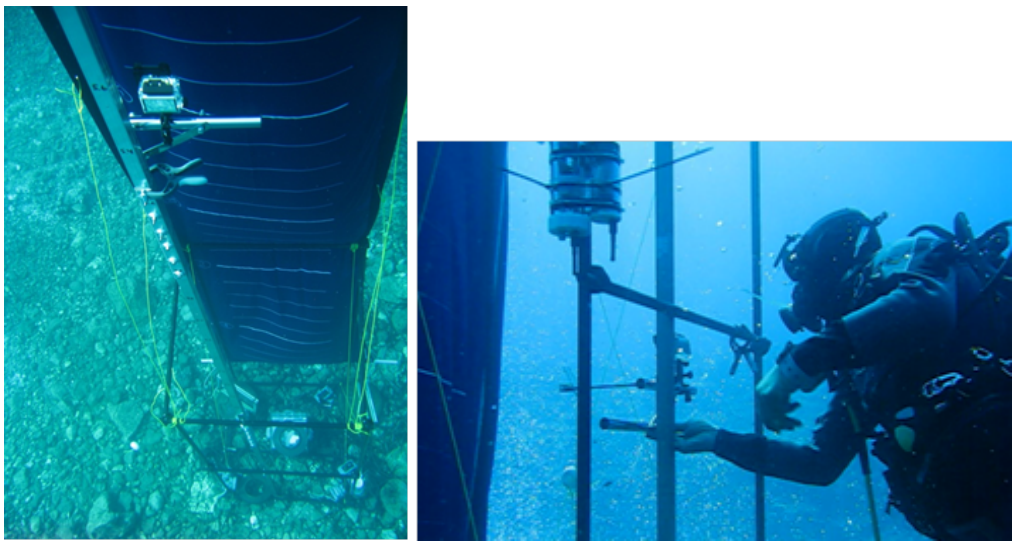

Figure 4: Photographs showing the experimental set-up for the UniRoma1 – OGS bubble dynamics measurements

The experiment involved release of the local gas (c. 95% CO_2) as 7 *mm* bubbles in a bubble train having bubbles about 1 every 20 *cm*. Bubble size was calculated by videoing rising bubbles accumulating on a Plexiglas sheet suspended at different heights above the bubble release point and measuring their diameter relative to graduated marks on the sheet. At least 20 bubbles per deployment height were measured and statistics calculated, with care taken to measure the bubble just before it hit the sheet to minimise the effect of deformation. Bubble size decreased in an almost linear manner before disappearing at about 2 m above the release point. Bubble rise velocity was calculated by measuring the velocity of individual bubbles over each 20 *cm* interval using 17 bubbles in various videos (which followed individual rising bubbles until they disappeared) and calculating appropriate statistics. Although variable, values averaged around 30 *cm/s*; the similar velocity despite changing bubble size implies the importance of the vertical current regime in influencing rise velocity in a natural system. Gas bubbles were collected at the same heights using a simple

funnel and glass vial, with samples analysed for CO_2, O_2, N_2, and CH_4. Water samples were collected by divers manually triggering Niskin bottles at the same height, with samples analysed for DIC, alkalinity, pH, and dissolved gases. In addition, CTD profiles were conducted at different times during the experiment and 2 GasPro-pCO_2 probes were deployed at different heights on the structure for the duration of the experiment to continuously monitor dissolved CO_2 and temperature. During the experiment, which lasted more than 3 hours, pCO_2 ranged from a minimum of 350 uatm to a maximum of 820 uatm.

In collaboration with D. McGinnis (IGB-Berlin) these data have been modelled using the Discrete Bubble Model (DBM), which was originally developed to predict oxygen transfer in artificial aeration systems in lakes and reservoirs (*McGinnis and Little, 2002*) and then later expanded to included methane (*McGinnis et al., 2006*) and CO_2 (*McGinnis et al. 2011*) bubbles. Based on an input gas concentration equal to that of the first bubble measured, the model was able to predict very well the subsequent gas bubble concentrations measured higher in the water column. In contrast, a higher concentration was needed to match the bubble diameter values, perhaps indicating that the field technique for this measurement requires refinement.

GEOMAR obtained field data encompassing optical, geochemical and current flow measurements to study CO_2 bubble dissolution and solute dispersion in a natural seepage setting. Bubble sizes and rise velocities were measured optically in high resolution from the seafloor to 80 cm above ground. Two cameras (Canon 5D Mark III and GoPro Hero III) and additional light were mounted on a vertical adjustable plate allowing the observation of bubbles during their ascent in 20 cm intervals. Simultaneously, water and gas samples were taken to analyze changes in gas bubble composition; solute gas concentrations (i.e. CO_2, O_2, N_2, H_2S) and total alkalinity in ambient seawater as a function of bubble raise height.

Additionally, CTD and current flow measurements were done in parallel to pCO_2 logging and were performed to study CO_2 solute dispersion under local physicochemical conditions and current forcing. During the campaign current directions were predominantly wind driven with a preferred SE component. Current velocities ranged from 0 - 15 cm/s with

an average velocity of ~ 7 cm/s indicating rather low current speed during the time of our campaign. pCO_2 values were measured 15 m to the south of the crater and showed highly elevated pCO_2 values. Maximal pCO_2 values were measured close to the seabed (0.5 m above ground) and exceeded a value of 10,000 µatm 15 m downstream of the seepage area. This indicates high gas emissions and low dilution of the solute in the absence of strong tidal cycles and at lower current velocities compared to a North Sea setting. Background pCO_2 (~420 µatm) was measured at ~ 3m water depth which coincides with the occurrence of a thermocline. First results of optical data indicate that the initial (at the seafloor) bubble size spectra are broad with bubble sizes ranging from 0.1 mm to >5 mm in radius. Further evaluation of image and geochemical data is currently in process. Data will be used to test parameterizations (i.e. rise velocity and mass transfer) used in numerical models.

4.3.2. The Gas release experiment in the North Sea

In summer 2012 (Expedition CE12010) *GEOMAR* conducted a gas release experiment at Sleipner in order to investigate the impact of CO_2 leakage under local tidal forcing and to test different geochemical monitoring devices. In 83 m water-depth carbon dioxide and krypton were released over 10 to 15 hours at varying gas fluxes (15- 50 L CO_2 min^{-1}; 1- 3 L Kr min^{-1}) and different initial bubble sizes. The impact of the gas discharge was observed in-situ during ROV dives and subsequent video-guided CTD casts using different geochemical devices (pCO_2 sensor, pH electrode, discrete water samples, and a membrane inlet mass spectrometer). Bubble sizes and rise heights were monitored optically using the HD-camera and sonar system of the ROV. The local current regime was measured with an ADCP. The experiment provides unique data on CO_2 bubble dissolution and solute dispersion under North Sea tidal forcing and oceanic conditions and is currently used to test and validate numerical models. Inter-comparison of varying geochemical devises is on-going to appraise their applicability for leak detection.

Maximal pCO_2 values were measured 50*cm* above the gas source, decreasing with increasing distance to the release spot. Unfortunately the experimental set-up influenced the local flow field by reducing the current velocities and by creating a pressure drop in the

flow shadow of the lander. Both significantly influenced solute dispersion and caused high pCO_2 values (reduced mixing and dilution) and the down welling of the solute CO_2 plume.

Due to strong tidal currents, and the fact that the gas flux of each experiment was temporally limited to 10-15 hours, the dissolved gas plume occurred only in the near-field and did not develop a measurable far-field component, which is however likely to be expected in natural vent areas or during a long-term leakage scenario.

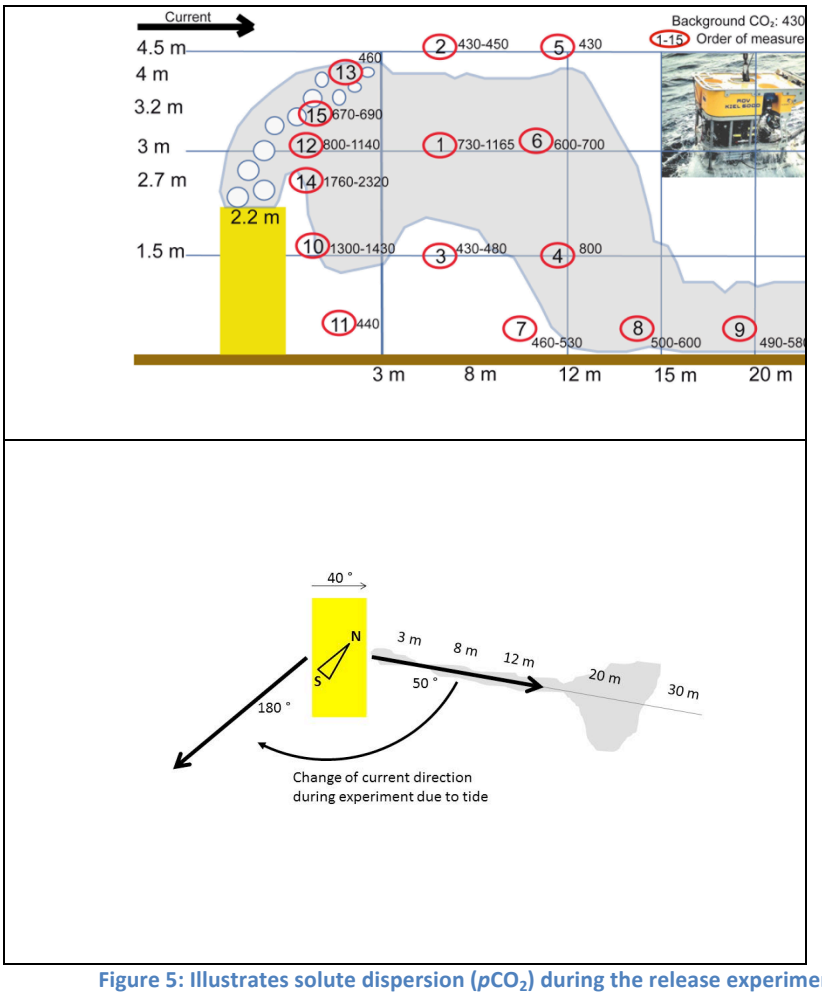

Figure 5: Illustrates solute dispersion (pCO_2) during the release experiment and the period of the ROV survey, which was conducted during a tidal turn. Model results show the shrinkage of CO_2 bubbles for a range of initial bubble sizes (d_e=2-8 mm). CO_2 is depleted after raising 2 m (d_e=4mm), which matches geochemical measurements and optical data of bubble sizes.

4.4. Conclusions bubble and plume

At Geomar numerical models are used to simulate the buoyant rise and dissolution of CO_2 bubbles in the water-column and the subsequent near-field dispersion of dissolved CO_2

in seawater under ocean current and tidal forcing. The corresponding pH change is calculated in a sub-model using measured CTD and TA data as well as modelled DIC data. In order to test and improve numerical models, fieldwork has been conducted within the Sleipner area (North Sea) and at a natural CO_2 seepage site off Panarea. Preliminary results indicate that the bubble dissolution model is able to track the rapid dissolution of gas bubbles during the release experiment very well. Simulations show that CO_2 is depleted after 2 m of rise (initial d_e=4mm), which coincides with geochemical measurements, and optical derived data of initial bubble sizes. However, the dissolution model significantly underestimates CO_2 depletion depths of natural CO2 bubbles seeping at Bottaro Crater, indicating that natural bubbles are faster and thus are able to transport CO_2 at shallower depth. Evaluation of optical data will provide information on the rise velocity of natural bubbles, which is the resultant of bubble slip velocity and entrained water speed. These new insights will be used to improve the parameterization of the rise velocity to extent the applicability of the bubble dissolution model from single bubble chains to bubble plumes (Task 3.3).

Similarly, modelling of the UniRoma1 / OGS experiments on bubble dynamics conducted at the Panarea test site have shown good agreement with observed results, although follow-up experiments are required to do more rigorous checks of input parameter sensitivity and model assumptions. The difficulty that remains, however, is being able to extrapolate single-bubble models to a real-world leak where gas is released in complex bubble trains of mixed sizes or at high flux rates where bubbles are irregularly shaped ellipsoids or caps that change dynamically during their rise. The interaction of bubble trains with the surrounding water column, and the more complex gas exchange dynamics for these larger, wobbling bubbles during their ascent (compared to those approximating a sphere) will require more complex modelling approaches.

Geochemical (pCO_2 and TA) and hydro-physical (current regime) data of the release experiment are currently being used to validate the plume dispersion model (task 3.3). The release experiment and modelling indicate that the impact of leakage at a rate comparable

to the experiment conducted at Sleipner (~130 kg/day) is limited to bottom waters (1-5 m above ground) and a small area around the gas source (50 m). Tidal cycles and strong currents significantly diminish the risk for the far-field of a leak, by efficiently diluting the solute in ambient seawater. Future modelling work at Geomar will encompass simulations of the spatial footprint in the near-field of a CO_2 leak under ocean current and tidal forcing and for varying leakage rates, which is linked to task 3.2.

Simulations of leakage bubble plumes and pH changes in the water column have been conducted by HWU for multiple scenarios and locations within the North Sea and surrounding waters, investigating how different parameters affect the bubble plume and pH changes of the seawater. The developed model was finely tuned using a combination of various on-site/near-site localised water parameters (currents, temperatures, salinity, depths, sediment size) along with the development of the bubble plume dynamics and dissolution through a number of sources with both laboratory and on-site/near-site experimental data analysis (initial bubble sizes, dissolution rates, rising velocities) detailed in D3.3.

To prepare for the North Sea scenarios to be simulated in, an example case study in a location similar to that of the Sleipner site has been performed. The case study is at ~100m depth, shown in the phase diagram *(*Figure 2), at this depth the leaked CO_2 is in gas bubbles with no hydrate formation. The average size of the bubble leaked is considered to be around 6*mm*. The leak is considered to be within the winter season with water currents of 10*cm/s* along the latitude direction. The leakage flux simulated is 46.35 $kg/day/m^2$ in a 15*m* x 15*m* area.

At this site, the bubble or droplet plume (with initial sizes of ~6.0mm) reached the terminal height of 2.81 within the first two and a half minutes of the leakage occurring as shown in the following figures. This rising distance is slightly greater than that of the Geomar experiment and model above, however this is to be expected due to the larger bubble size taking longer to dissolve. However, there is still a relatively fast dissolution rate, and with the fast dissolution there is a greater change in pH in a small volume, with the maximum

change of -2.0 recorded in a one-hour period. The total volume of fluid with change in pH greater than 1.5 is about 2500m^3, total volume of fluid with change in pH greater than 1.0 is about 6500m^3, and the total volume of fluid with change in pH greater than 0.5 is about 9100m^3. Further details, scenarios and comparisons of changing parameters on the model may be seen in D3.3

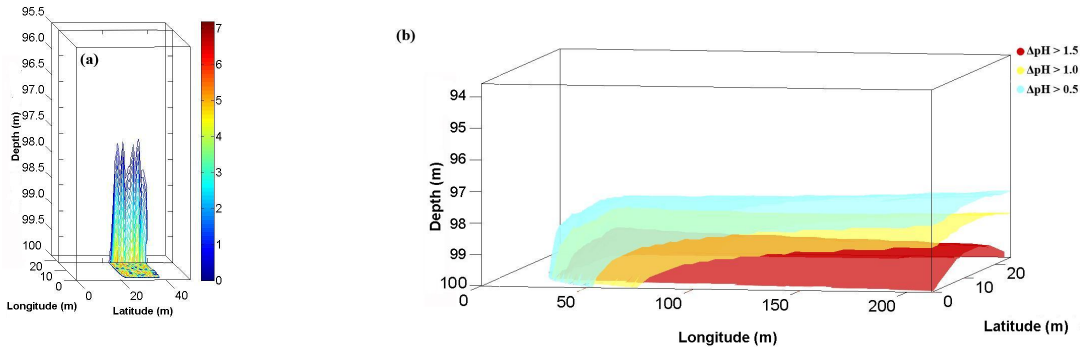

Figure 6: a) average bubble diameter (mm) during dissolution for the rising bubble plume. b) change in pH of the localised waters.

5. Part II: Hydro-acoustics

5.1. Introduction

Multibeam echo sounders (MBES) and single-beam echo sounders (SBES) are potent tools to image both the water column and seabed. SBES have been used for many years in fisheries research, and can be used to identify the presence/absence of bubbles within a typical 10-degree beam footprint. MBES systems are used to collect high-resolution seafloor profiles across a swath typically 2-2.5x the water depth. Multibeam systems can also be used to acquire water column information, giving the full 3D shape of rising bubble plumes and fish schools.

5.2. Data collection

5.2.1. Bathymetry

Bathymetry is typically collected using a MBES. The R/V G.O. Sars, R/V James Cook, and R/V Alkor have an EM302, EM710, and Seabeam 1000 respectively. All of these MBES systems are fully capable within the depth range of 100 m-1000 m applicable to this project. Proper technique in acquisition, quality assessment, and processing is essential to the creation of an accurate MBES data product. The key factors contributing to a quality survey are: the sound velocity profile, monitoring of the acquisition software, and grid-wide crossing lines for syn-acquisition reference.

The most important factor in the collection of acoustic soundings is the sound velocity profile (SVP). The sound structure informs ray-tracing algorithms in the acquisition software, and is used in real-time to accept or reject soundings used by the bottom-lock algorithms. In the open ocean the SVP is relatively stable, and a single CTD or expendable bathythermograph (XBT) deployment at the beginning of a survey is more than sufficient to acquire quality data. In places with complex topography, especially in regions of high relief with respect to the surrounding terrain, the SVP may only be stable for a matter of hours.

Knowledge of the region to be surveyed is essential to estimate the frequency of SVPs that will need to be collected.

SVPs are always collected before every survey, typically by CTD or XBT deployment. The CTD gives a much more detailed profile, but will take much longer for deployment and recovery. The XBT collects only temperature information, but can be deployed and input into the acquisition software in a matter of minutes while underway. The number of SVPs to collect is dependent on the survey region, and varies from a single profile per day to a profile every few hours. Each survey must be planned for the region surveyed, and be adaptable.

Each survey should begin with a line perpendicular to the main survey direction, and spanning the entire survey range. This first line should be a narrow swath line with at most ±50˚ off nadir to minimize SVP error. This line will be used as a stable reference with the best possible SVP for all other lines collected during the survey. Each subsequent line can be compared in real-time on the acquisition system screen to this first line. The operator is looking for the vertical and horizontal offset of the outer beams of the survey lines with respect to the near-nadir collection of the crossing line. If the outer beams show a significant offset, for example more than 3 m in 700 m water depth, the SVP is no longer accurate and needs to be re-acquired.

Inherent in a good survey is the monitoring of the acquisition equipment and record keeping during acquisition. Abnormalities in the bottom lock and water column profile are simple to diagnose and correct during acquisition, but impossible to correct in post-processing. A knowledgeable technician must be monitoring the collection at all times and ready to respond to changes in survey conditions to optimize collection. Additionally a written record of the survey, acquisition settings, and integration of each new SVP must be maintained. The Kongsberg raw.all file format stores the input SVP, but without any metadata on that input. It is possible to replace a bad SVP and recover survey data that would otherwise be lost, but only if a record of each SVP were made.

5.2.2. Water column

Water column acoustic data can be collected with both multibeam and single beam echo sounders. With SBES an average sound velocity is derived from the most recent SVP

and applied to the acquisition system. The SBES provides a vertical profile of the water column, and in a typical installation such as the Kongsberg EK60, the system is calibrated to signal return from a known target. This provides a detailed look at the water column and a possible estimate of the flux of volume scattering elements from a single bubble plume. This however is difficult to reconcile with the flux of gas from the seafloor as the SBES typically provides a large beam angle of 10 degrees, though the split-beam capability significantly improves horizontal resolution. The large footprint of most SBES systems make these reasonable for viewing small gas seeps, and potentially for quantifying the flux of gas from discrete vents but not a compilation of venting areas.

MBES systems provide multiple beams in a cross-path swath. These systems are very tightly resolved in narrow beams, typically 0.5-1 degree in cross-path and along-path resolution. The array of narrow beams in MBES systems, when they are sensitive to water column returns, provides a swath of coverage equal to the depth to seafloor at first contact to bottom. The MBES requires an up to date SVP as all outer beams must be ray-traced through the water column. Use of an old SVP or an average sound speed for the water column will result in very poor sensor acquisition and system stability. The useable swath for water column is limited due to side lobe interaction with the bottom, as the water column returns are several orders of magnitude weaker than the primary bottom return. While a limiting factor, MBES can still image a water column swath equal to the depth to bottom, which in the Sleipner will be 80-90 m and at Jan Mayen is in excess of 500 m. This is a dramatic improvement over the SBES swath, especially considering that the range imaged is broken into narrow discrete beams rather than integrated into a single image.

5.2.3. Quantification of bubble flux

It is not possible to quantify bubble flux from top-down MBES without a clear knowledge of the dynamics of each vent and a calibrated multibeam system. Even with the resolution of a multibeam echo sounder the system can only resolve a discrete amplitude return from a given volume of water. Without a calibration of that amplitude return with respect to the bubble present in the water column it is not possible to estimate the flux.

SBES systems, especially split-beam systems such as the commonly installed Kongsberg EK60 series, are potentially sensitive to the calculation of bubble flux. These systems, when coupled with water column velocity estimates from an ADCP system, can be used to estimate the bubble velocity and calibrated return strength. For small venting systems with discrete bubble trains it should be possible to estimate the volume of gas escaping from the system (*Muyashkin and Sauter 2010*). This method assumes that the bubble size distribution is larger than the resonance size of a bubble for the given acoustic system, which has been shown to be true for free gas at a depth range of 0-1000m (*Greinert and Nutzel, 2004*) and is not affected by the presence of methane hydrate skins (*Muyakshin and Sauter, 2010; Maksimov and Sosedko, 2009*).

In the summer 2014, a new technique to quantify bubble flux from the seafloor by using a Lander system will be tested by the Center for Geobiology (UiB). The Lander uses a Kongsberg EK60 side-looking sonar system calibrated to known bubble volumes to estimate the flux from a single vent or a set of closely spaced vents within the splitbeam range angular range.

5.2.4. Distinguish CO_2 and CH_4 bubbles

It is possible to distinguish the gas content of bubbles based on their terminal rise velocity. Methane rises approximately 70% faster than CO_2 in small discreet bubbles (Bigalke et al. 2010). To date however, no single system has been used to successfully quantify the rise velocity of bubbles in the water column with enough accuracy to calculate the chemical composition of the bubbles. This is due to the numerous complications, namely the water column velocity structure, buoyant plumes of bubbles with rising water mass entrainment, and the limited vertical resolution of top-looking sonar systems. While challenges exist in determining the terminal rise velocity, the Centre for Geobiology (UiB) in the summer of 2014 will deploy AUV-based high resolution MBES with high vertical resolution capability. This coupled with well-mapped bubble vent locations at the Jan Mayen vent field will allow for the first-ever accurate assessment of the velocity structure of rising bubble plumes from a hydrothermal CO_2 vent site.

5.2.5. Limitations

The limitations on collecting acoustic data vary by vessel, acquisition system, and the level of care used in setting up a survey. The most common limitation on acquisition is the co-collection of MBES, SBES, and sub-bottom profiling while performing survey work. In some instances, especially when a timing delay slave-master system is used, successful SBES and MBES data can be collected without degrading the data quality of either system. This however is rare, as purposeful monitoring of the acquisition systems requires skilled personnel onboard and working during the survey. Typically MBES and SBES systems are run concurrently, mutually interfering with each other and degrading the image and signal quality of the respective systems. This provides marked challenges to subsequently process the data, and in some cases makes identification of water column features in the MBES impossible due to the level of interference. That said, interaction of MBES and SBES typically does not damage the MBES signal to the point that it interferes with the collection of bathymetric data, though this is possible.

It is not possible to concurrently run a sub-bottom profiler and either MBES or SBES and collect high quality data on either of the latter systems. On the ships used during these investigations the R/V G.O. Sars and R/V Alkor both have parametric subbottom profilers. Parametric systems are acoustically very powerful, and completely destroy the STN ratio of any other echosounder running concurrent to subbottom profiler acquisition. For any useable MBES data to be collected, it must be run entirely independent of a subbottom parametric system to obtain a high quality of data collected.

5.3. Results from ECO2-expeditions

5.3.1. Jan Mayen vent fields

The R/V G.O. Sars cruised to the Jan Mayen vent fields in the summer of 2011, 2012 and 2013. A main feature of the Jan Mayen vent fields is the high CO_2 concentrations of the venting fluids. Pedersen et al. (2010) measured endmember CO_2 concentrations of up to 92 mmol/kg in the high-temperature vent fluids. In 2011, the composition of bubbles released from the seafloor at the main Troll Wall vent field was determined by the same research

team. They found that CO_2 was the main constituent of these bubbles (about 80 % CO_2).

Both cruises, in 2012 and 2013, collected multibeam and single-beam echosounder profiles over the main Troll Wall vent field, making passes both parallel and perpendicular to the cliff face that comprises the Troll Wall field. The 2012 data was somewhat compromised by the concurrent use of an EK60 single beam echosounder used without a timing delay system which resulted in systematic interference of the multibeam system, especially in the water column image. The 2013 data collection, though hampered for most of the time by high winds and large NE swell, collected numerous passes of high quality water column returns of the Troll Wall bubble plumes, giving clear indication of their rise heights, plume structure, and occurrence of plumes along the Troll Wall venting system (Figure 6 and Figure 7).

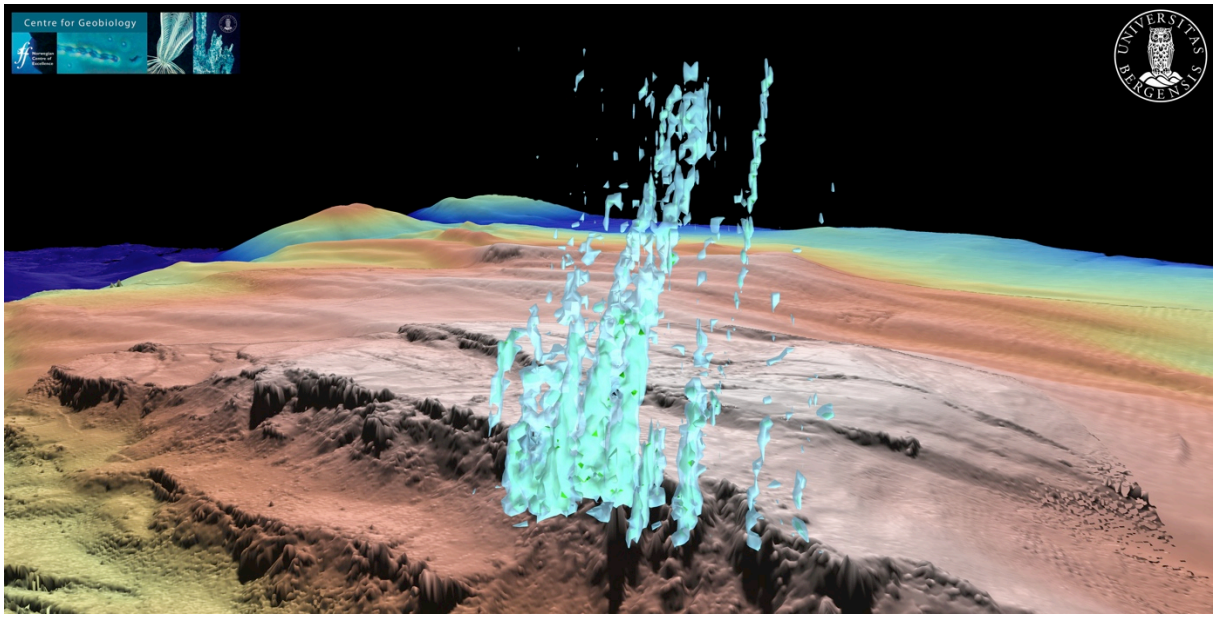

Figure 7: Image of the Troll Wall venting system, as a compilation of several MBES survey lines and gridded as an iso-amplitude volume.

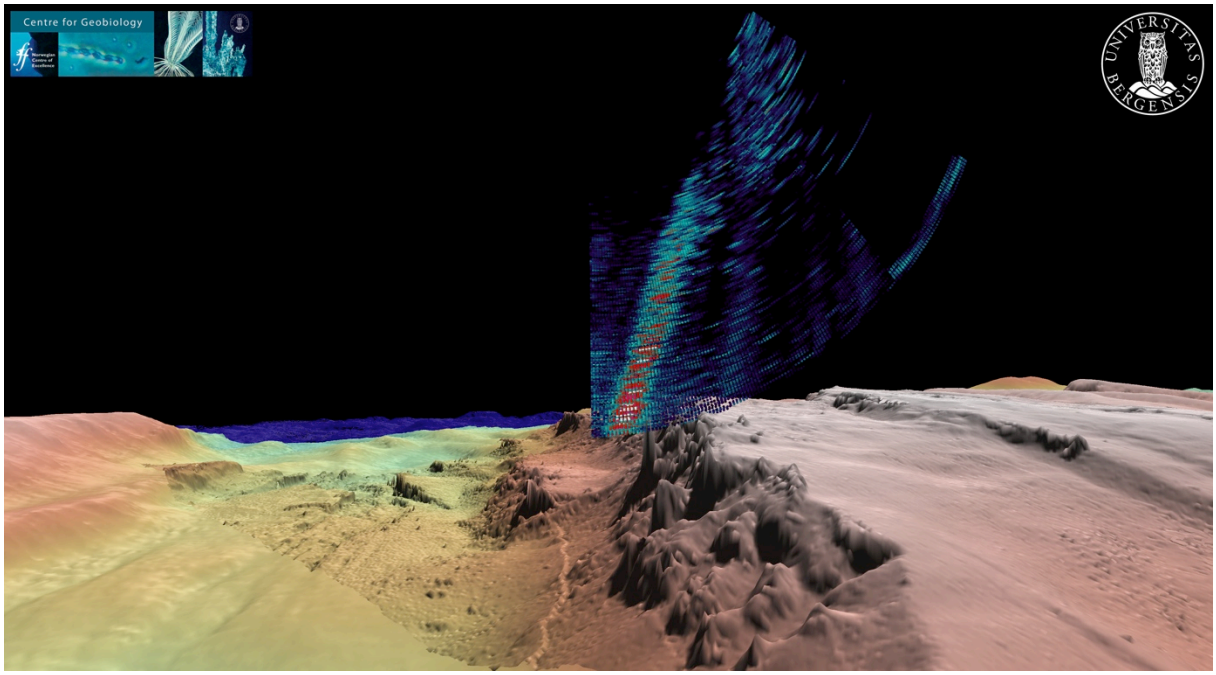

Figure 8: Single ping profile of the Troll Wall venting, this demonstrates the horizontal resolution achievable with MBES and the plume shapes that can be seen with this system.

Given the images of bubble plumes at Troll Wall and at other shallow hydrothermal venting systems it is apparent that MBES are appropriate for both continued imaging of bubble plumes in the water column and also for the discovery of shallow hydrothermal or gas seep systems.

5.3.2. Panarea (PaCO2)

Hydroacoustic Mapping of gas seepage at Panarea: Acoustic measurements performed during the Urania cruise under the umbrella of PaCO2 in 2011 yielded novel acoustic data of high quality. Thus a new gas-seep distribution map could be acquired for the study area, demonstrating that the seepage areas are much larger than previously assumed. In contrast to the research proposal, the in situ hydroacoustic monitoring device GasQuant was not available for the cruise. Alternatively, we rented a very modern, state- of-the-art high frequency multibeam sounder (R2Sonic 200-400kHz) with a prototype water column imaging functionality. The device delivered exceptionally high quality data and even individual bubble streams could be resolved. These data have already been partially presented in Schneider von Deimling and Papenberg (2012). Further data processing of the

R2Sonic data together with ADCP results will finally allow for gas flux estimates and determination of the bubble dissolution dynamics during ascent through the water.

Records of the subbottom chirp data have been reviewed, showing a maximum seafloor penetration of 10m. Once all sub-bottom acoustic data have been processed, bathymetry has been cleaned, and all gas ebullition sites have been mapped, we will link these data to investigate potential geologic control of the gas emissions.

The high-resolution hydroacoustic data described above was successfully used to accurately choose locations of interest for water sampling, including both leak and non-leaking sites. Besides sampling, identified seep sites were further explored using R/V Urania's ROV, a Geitaliana Pollux Tre.

The main goal of the acoustic studies was to detect CO_2 bubbles emitting from the seafloor and in the water column. Thus, the overall subseafloor gas distribution, quantitative mapping of ebullition sites and determination of respective gas bubble rise heights could be constrained. Unfortunately, R/V Urania's sparker system was damaged and sent for repair prior to the PaCO2 cruise. Instead R/V Urania's chirp system was operated during the cruise. Due to the shallower penetration depth of the chirp compared to that of a sparker system, subbottom imaging was limited.

5.3.3. Sleipner

The R/V G.O. Sars visited the Sleipner area in 2012, collecting multibeam and single-beam echosounder data. In addition to the G.O. Sars, the R/V James Cook and R/V Alkor collected multibeam and single beam data in 2013. All of the cruises collected data that is not useable for water column or multibeam mapping purposes. This was due to a variety of acquisition errors, most commonly errors in software setup, or the concurrent collection of data on systems that strongly interfere with MBES acquisition.

5.4. Hydroacoustics as monitoring tool

From the Jan Mayen vent fields and Panarea site it is clear that MBES is a powerful

tool for determining the occurrence and dynamics of bubble plumes in the water column. Given the dramatically improved survey swath provided by MBES over SBES, the MBES is much more efficient in surveying for seafloor gas seeps. In addition to locating the seeps the concurrent acquisition of bathymetric soundings provides a detailed look at the seafloor features that may be related to the gas seeps. SBES systems are appropriate for examining time-series on a single location, and could be used to calculate the rise velocity of bubbles from a single source, but given the narrow water column region surveyed by the single beam these systems are not appropriate for locating gas seeps on the seafloor.

While MBES systems are powerful tools for locating seafloor gas seeps, they work best on dedicated water column surveys and are highly susceptible to interference from other acoustic systems. MBES surveys run concurrent with SBES systems must be set up with timing offsets to prevent signal interaction. As well, it is not possible to run MBES and sub-bottom profiling parametric systems concurrently. With these stipulations, multibeam sonar systems have the potential to provide the highest resolution, fastest, and consequently least expensive method for monitoring for potential gas seeps possible with current technologies.

6. Part III: The Carbonate System

6.1. Introduction

WP3, entitled "Fate of CO2 and other Gases emitted at the Seabed", focuses on the chemical, biological, and physical mechanisms that control CO_2 within the water column. Thus, at least one of four main parameters of the carbonate system in seawater was often measured during the ECO2 cruises. *Zeebe & Wolf-Gladrow* (2001) provide a detailed account of the equilibria and kinetics of the carbonate system. For a complete description of this system two of the following four parameters must be measured: dissolved inorganic carbon (DIC), Alkalinity (Alk), pH, and partial pressure or fugacity of CO2 (pCO2 or fCO2). The remaining two parameters can then be computed from equilibrium equations and thermodynamic constants using standard software like CO2sys.

This chapter provides an overview of the carbonate system measurements obtained in the water column during the ECO2 cruises (Table1). Our aim is to (i) synthesize technical information and preliminary results that has been scattered in different cruise reports (ii) document the quality of different measurement techniques and resulting data, and (iii) attempt to draw a general conclusion on the fate of CO2 emitted at the Seabed.

6.2. Methods

Most of the surveys that have been carried out during the extensive ECO2 cruise program (Table 1) obtained samples and/or measurements for the seawater carbonate system. An overview of the sampling area, measurement parameters, and contact persons is given on Table 2.1. These measurement campaigns had different objectives and were conducted by various institutions. Therefore a suit of different sampling methods and measurement techniques were utilized.

A discrete, CTD-based sampling was often used for water column DIC and Alk, and

occasionally for pH. Niskin water samplers were fired at selected depth and locations during CTD tracks and casts. Seawater samples were transferred from Niskin bottles to 250-500 ml glass bottles and analysed either on-board or at the laboratories on land. In the latter case the samples were normally poisoned by adding a saturated HgCl2-solution in order to prevent contamination by biological activity. All the above discrete sampling methods involve some bottling and thus will be denoted by B in Tab 2.1.

A continuous sampling method coupled with different sensors for seawater pCO2 (or fCO2) was utilized for the determination of dissolved CO2 gas in the seawater. The following sensors were used for this purpose:

a) HydroC instrument from Contros. This sensor has the capability to be mounted to the CTD frame and record profile data online during CTD stations. To allow the sensor's internal temperature to reach thermal stabilisation, the pCO_2 sensor was powered-up half an hour before the CTD tracks began. It can measure in situ within 0-4000m with analysis time of 1 seconds and accuracy of ± 1 %.
b) A highly accurate instrument (± 2 µatm) which measures the surface seawater fCO_2. This instrument uses a non-dispersive infrared (NDIR) CO2/H2O gas analyzer (from LI-COR) to determine the CO_2 concentration in a headspace air in equilibrium with a continuous stream of seawater (e.g. Feely et al. (1998).
c) pCO2 (Microelectrodes Inc., USA)….

Water column concentration of DIC was determined by:

a) the coulometric titration method (e.g. Johnson et al., 1993) using a VINDTA instrument (ref). The accuracy was set by running Certified Reference Material (CRM) supplied by Andrew Dickson at Scripps Institute of Oceanography, USA.
b) Non-dispersive infrared measurement (NDIR) using Shimadzu TOC-V CSH analyser

Water column Alkalinity was determined by:

a) titrating samples with 0.1 M HCl as described by Haraldson et al. [1997] using a

VINDTA instrument. The accuracy was set in the same way as for DIC.

b) By open cell potentiometric titration with 0.1 M HCl as described by Dickson et al. (2007a) using a Mettler Toledo G20 Titrator

Water column pH was determined by using:

a) A custom, bench-top, flow-cell based spectrophotometric pH detection system developed at the Geophysical Institute, UiB. The precision (±0.001 pH) and accuracy (±0.005 pH) was determined from comparison with certified reference material. The results were expressed on the pHT scale.

b) By spectrophotometry (indicator: m-cresol violet) with a Varian Cary 50 spectrophotometer with thermostatted cylindrical cell holders maintained at 25.0°C according to Dickson et al. (2007b). The results were expressed on the pHT scale; the in situ pH was calculated using pressure, temperature and salinity measured by the CTD probe.

c) SBE27-pH sensor (SBE in Table 2.1). This sensor is less accurate (±0.1 pH units), but it can take profiles.

d) A pH 96 by WTW (Wissenschaftlich-Technische Werkstätten GmbH, Weilheim, Germany) and an InLab Semi-Micro electrode by Mettler Toledo (Gießen, Germany). Samples were cooled to in situ temperature (19°C) before measuring pH. Calibration was done with conventional buffer solutions by Mettler Toledo (pH 4.00 and 7.00).

e) A WTW Inolab Level 2 pH-meter with a Sentix 81 glass electrode having a precision of +/- 0.005. The pH-meter was calibrated at pH 4.01, 7.00 and 9.00 before each set of analyses with conventional Mettler Toledo buffer solutions.

f) A Mettler Toledo G20 Titrator using an electrode DGi115SC at controlled temperature (25.0 °C).

g) ISFTET sensor developed at Kyushu University (Shitashima et al., 2013). I can measure *in situ* within 0-3000m with analysis time of 1 seconds and accuracy of ± 0.005 pH units.

At the moment it is unclear whether all the above pH measurements are on the total scale and can be directly compared to each other.

Cruise	Area	DIC	Alk	pH	pCO2/fCO2	Contact person
ALKOR cruise 374	1,2	b	b	c	a	P. Linke, GEOMAR plinke@geomar.de
AL412 (22.03.-08.04.2013, by GEOMAR)	1	**a**	**a**	**c**	**a**	P. Linke, GEOMAR plinke@geomar.de
St. Barbara (June-Sep 2012, by ?? Poland)						
R/V G.O. Sars (23-30 June 2012)	1	a	a			A. Omar abdir.omar@uni.no
R/V G.O. Sars (3 July –04 August 2012)	4	a	a			A. Omar abdir.omar@uni.no
ECO2-2 (Panarea Island, Italy)	3					
ECO2-4 (Panarea Island, Italy)	3					
ECO2-6 (Panerea)	3					
RV CELTIC EXPLORER (20.07. – 06.08.2012)	1	**a**	**a**	**c**	**a**	P. Linke, GEOMAR plinke@geomar.de
JC077 (2ND - 28TH September 2012)						
PaCO2 (27 July – 01 August 2011) (Panerea)	3					

Table 6.1 Overview of the carbonate parameter measurements in ECO2 and their corresponding sampling method and measurement techniques. Numerals 1-5 denote the four study sites within ECO2 i.e.,Sleipner, Juist seep, Panarea, Jan Mayen vent fields and the Okinawa Trough, respectively. Letters denote sampling methods and measurement technique as explained in the main text.

6.3. Results from ECO2-expeditions

6.3.1. Sleipner

During the cruise programs focusing on the Sleipner area a large number of CTD stations were occupied guided by geophysical data and chemical and physical data obtained from ship and AUV surveys. There was no CO_2 seepage detected but many sites of methane leakage were found, associated with either abandoned well heads or fractures such as the Hugin fracture.

Discrete water samples were taken in the Sleipner area during CTD casts in summer 2012. Bottom water alkalinity (TA) remained rather constant at 2.332(5) meq/l. Background pCO_2 was around 430 µatm corresponding to a DIC (dissolved inorganic carbon) of 2.17 mM. Boron and calcium concentrations within bottom waters were 0.4 mM and 10.4 mM, respectively. The geochemical measurements are used to determine the carbonate system in the Sleipner area and are crucial to simulate the corresponding pH during potential seabed leakage of CO_2.

6.3.2. Salt Dome Juist

Gas bubbles were observed in areas where strong acoustic flares, low pH and high concentrations of CO2 were determined near the seafloor (*McGinnis et al*., 2011).

6.3.3. Panarea

UniRoma1 and OGS have performed a complete suite of carbonate system parameter analyses on water samples coming from benthic chambers and from the water column in and around the CO2 seep areas. In cases where a complete suite of parameters was measured it was possible to test internal consistency and method accuracy by using two parameters to calculate a third using the software package CO2Calc (Robbins et al., 2010). Results of these tests showed excellent results, with the standard headspace technique for

pCO2 analyses showing, as expected due to the manual nature of the method, the largest error (c. 5%). Experiments involving the co-deployment of a GasPro-pCO2 probe on a pH meter equipped CTD were also conducted to examine the correlation between the two sensors; the overall correspondence was good, but the almost instantaneous response of the pH meter was, as expected, much faster than the diffusion controlled response of the GasPro. Work is underway to combine units and decrease response times.

UniRoma1 was also involved in high-frequency spatial monitoring of pCO2 and temperature through the deployment of 20 GasPro-pCO2 units along a vertical water-column profile located 3m from the same leaking pockmark. The profile was oriented perpendicular to the pockmark main axis, and perpendicular to the main current direction. The probes were programmed to measure once every 10 minutes and were deployed over a 2.5 day period. This work was performed to study mixing and transport dynamics of CO2 once it had been dissolved into the water column. Although this data is still being processed, initial interpretation shows dynamic motion of water with anomalous values (pCO2 <1500 uatm) moving across the transect in a background field with values <500 uatm, as well as at least 4 events where water with strongly anomalous pCO2 values (4000 to 7000 uatm) move across the transect. Of these 4 events, two different styles can be observed. The first is where the anomalous water is restricted to the bottom 2 m of the water column, resulting in a strong vertical pCO2 gradient. This matches well with the stratified conditions observed during the campaign, and also the bubble dynamic experiments described above which indicate that the majority of the CO2 is dissolved in the first few metres above the sediments. The second involves a strong anomaly first forming at a height of 2 m above the sediments (at two adjacent probes), which then moves slightly downwards before dissipating. This latter may indicate fingering and may be linked to vertical shear or to density flows generated by the bubble column. pCO2 results are presently being compared to the temperature and pressure (i.e. tide) data for a more complete interpretation. Unfortunately it was not possible to deploy an ADCP current meter during this period as planned; however more complete experiments are planned for the near future.

6.3.4. Jan Mayen vent fields

GFI and Uni Research analyzed water column samples for DIC and Alk during R/V G.O. Sars (23 July –04 August 2012). Preliminary results show extremely high DIC concentrations in the bottom water immediately surrounding the vents. Furthermore, comparison between DIC profiles obtained at a reference station with those obtained over the vents shows a slightly higher DIC concentration in the latter area. However, in order to separate the effect of the venting CO2 on the DIC concentration other physical and biological processes must be taken into account. This analysis is underway. Alkalinity data do not reveal any difference at the vents area compared to the reference station.

6.4. Conclusions

High carbon concentrations and/or low pH have been reported from all sites where natural seepage of CO2 occurs whereas at Sleipner, where industrial subsea CO2 storage exits, only normal background values have been observed. Hence, the few available results so far indicate that measurements of the carbonate system in the water column are suitable for quantification of the effects of seepage on the water chemistry. For the detection/localization of seepage, on the other hand, some other supplementary parameters need to be measured in addition to carbonate system parameters.

7. References

Alendal, G., and H Drange. 2001. "Two-Phase, Near-Field Modeling of Purposefully Released CO_2 in the Ocean." *Journal of Geophysical Research-Oceans* 106: 1085–1096.

Aliani, S., G. Bortoluzzi, G. Caramanna, and F. Raffa. 2010. "Seawater Dynamics and Environmental Settings After November 2002 Gas Eruption Off Bottaro (Panarea, Aeolian Islands, Mediterranean Sea)." *Continental Shelf Research* 30 (12) (July): 1338–1348. doi:10.1016/j.csr.2010.04.016.

Aya, I., Yamane, K., Nariai, H., (1997). Solubility of CO_2 and density of CO_2 hydrate at 30 MPa. Energy 22, 263–271.

Bigalke, N K, L I Enstad, G Rehder, and G Alendal. 2010. "Terminal Velocities of Pure and Hydrate Coated CO_2 Droplets and CH4 Bubbles Rising in a Simulated Oceanic Environment." *Deep-Sea Research Part I* 57 (9) (January 9): 1102–1110. doi:10.1016/j.dsr.2010.05.008.

Bigalke, N. K, G. Rehder, and G. Gust. 2008. "Experimental Investigation of the Rising Behavior of CO_2 Droplets in Seawater Under Hydrate-Forming Conditions." *Environmental Science and Technology* 42 (14): 5241–5246. doi:10.1021/es800228j.

Blackford, J. C., S Widdicombe, D Lowe, and B Chen. 2010. "Environmental Risks and Performance Assessment of Carbon Dioxide (CO_2) Leakage in Marine Ecosystems." In *Developments and Innovation in Carbon Dioxide (CO2) Capture and Storage Technology, Volume 2 - Carbon Dioxide (CO_2) Storage and Utilisation.*, edited by M. Mercedes Maroto-Valer, 344–373. Woodhead Publishing Limited.

Bozzano, G, and M Dente. 2001. "Shape and Terminal Velocity of Single Bubble Motion: a Novel Approach." *Computers and Chemical Engineering*.

Bozzano, G, and M Dente. 2009. "Single Bubble and Drop Motion Modeling." *Chemical Engineering* 17: 5gy.

Brennen, C. 1995. *Cavitation and Bubble Dynamics*. Oxford University Press.

Brewer, P G, ET Peltzer, G Friederich, and G Rehder. 2002. "Experimental Determination of the Fate of Rising CO_2 Droplets in Seawater." *Environmental Science and Technology* 36 (5441-5446): 4.3.

Caramanna, G, and N Voltattorni. 2011. "Is Panarea Island (Italy) a Valid and Cost-Effective Natural Laboratory for the Development of Detection and Monitoring Techniques for Submarine CO_2 Seepage? - Caramanna - 2011 - Greenhouse Gases: Science and Technology - Wiley Online Library."

Chen, B. , Y Song , M Nishio, M and M Akai (2003) Large-eddy simulation of double cloud formation induced by CO_2 dissolution in the ocean. *Tellus*, Ser. B **55**, pp 723--730

Clift, R., J R Grace, and M E Weber. 1978. *Bubbles, Drops, and Particles*. *Academic*. Academic Press, Inc.

Dewar, M, W Wei, D McNeil, and B Chen. 2013. "Small-Scale Modelling of the Physiochemical Impacts of CO_2 Leaked From Sub-Seabed Reservoirs or Pipelines Within the North Sea and Surrounding Waters." *Marine Pollution Bulletin*.

Drange, H, G. Alendal, and OM Johannessen. 2001. "Ocean Release of Fossil Fuel CO_2: a

Case Study." *Geophysical Research Letters* 28: 2637–2640.

Feely, R. A., Wanninkhof, R., Milburn, H. B., Cosca, C. E., Stapp, M., and Murphy, P. P. 1998: A new automated underway system for making high precision pCO2 measurements onboard research ships, Anal. Chim. Acta, 377, 185–191.

Gangstø, R, P.M Haugan, and G Alendal. 2005. "Parameterization of Drag and Dissolution of Rising CO_2 drops in Seawater." *Geophysical Research Letters* 32 (10): 4. doi:10.1029/2005GL022637.

Greinert, J., B. Nutzel (2004). Hydroacoustic experiments to establish a method for the determination of methane bubble fluxes at cold seeps. *Geo-Marine Letters*, v. 24 pp. 75-85, doi: 10.1007/s00367-003-0165-7.

Haraldson, C., L. G. Anderson, M. Hasselov, S. Hulth, and K. Olsson, 1997. Rapid, high-precision potentiometric titration of alkalinity in the ocean and sediment pore waters, Deep Sea Res., Part I, 44, 2031– 2044.

Hvidevold, H. K., G. Alendal, T. Johannessen, and T. Mannseth. 2012. "Assessing Model Parameter Uncertainties for Rising Velocity of CO_2 Droplets Through Experimental Design." *International Journal of Greenhouse Gas Control* 11 (November 1): 283–289. doi:10.1016/j.ijggc.2012.09.008.

Hvidevold, H. K., G. Alendal, T. Johannessen, and T. Mannseth. 2013. "Assessing Model Uncertainties Through Proper Experimental Design." *Energy Procedia* 37 (January): 3439–3446. doi:10.1016/j.egypro.2013.06.233.

Johnson, K. M., Wills, K. D., Butler, D. B., Johnson, W. K., and Wong, C. S.: 1993 Coulometric total carbon dioxide analysis for marine studies: maximizing the performance of an utomated gas extraction system and coulometric detector, Mar. Chem., 44, 167–187.

Leifer, I, and R K Patro. 2002. "The Bubble Mechanism for Methane Transport From the Shallow Sea Bed to the Surface: a Review and Sensitivity Study." *Continental Shelf Research*.

Maksimov, A. O., Sosedko, E.V. (2009). Acoustic manifestations of gas hydrate shelled bubbles. *Acoustical Physics*, v. 55 no. 6, pp. 776-784, doi:10.1134/S1063771009060128.

Mcginnis, D. F., and J. C. Little (2002), Predicting diffused-bubble oxygen transfer rate using the discrete-bubble model, *Water Research*.

McGinnis, D.F., Greinert, J., Artemov, Y., Beaubien, S.E., Wuest, A., (2006). Fate of rising methane bubbles in stratified waters: How much methane reaches the atmosphere? J. Geophys. Res. 111, C09007, doi:10.1029/2005JC003183.

McGinnis, D.F., Schmidt, M., DelSontro, T., Themann, S., Rovelli, L., Reitz, A., Linke, P., 2011. Discovery of a natural CO_2 seep in the German North Sea: Implications for shallow dissolved gas and seep detection. Journal of Geophysical Research: Oceans 116, C03013.

Mori, Y.H., Mochizuki, T., (1998), Dissolution of liquid CO_2 into water at high pressures: a search for the mechanism of dissolution being retarded through hydrate-film formation. Energy Convers. Manage. 39 (7), 567–578.

Muyakshin, S. I., E. Sauter (2010). The hydroacoustic method for the quantification of the gas flux from a submersed bubble plume. *Oceanology*, v. 50 no. 6, pp. 995-1001, doi: 10.1134/S0001437010060202.

Pedersen, R. B., I. H. Thorseth, R. E. Nygård, M. D. Lilley, D. S. Kelley (2010), Hydrothermal activity at the arctic mid-ocean ridges, in *Diversity of hydrothermal systmes on slow spreading ridges, Geophys. Monogr. Ser.*, vol. 188, edited by P. Rona et al., pp. 67-90, AGU, Washington D. C.

Rehder, G., P. W. Brewer, E. T. Peltzer, and G. Friederich (2002), Enhanced lifetime of methane bubble streams within the deep ocean, Geophys. Res. Lett., 29(15), 1731, doi:10.1029/2001GL013966.

Schneider von Deimlig, J. and C. Papenberg (2012), Detection of gas bubble leakage via correlation of water column multibeam images, in *Ocean Sciences*, vol. 8 pp. 175-181, doi: 10.5194/os-8-175-2012.

Robbins, L.L., Hansen, M.E., Kleypas, J.A., and Meylan, S.C., 2010, CO2calc—A user-friendly seawater carbon calculator for Windows, Max OS X, and iOS (iPhone): U.S. Geological Survey Open-File Report 2010–1280, 17 p.

Sato T. and K. Sato, (2002) Numerical prediction of the dilution process and its biological impacts in CO_2 ocean sequestration*J Mar Sci Technol* **6**, 169.

Shitashima, K., Y. Maeda, and T. Ohsumi, 2013. Development of detection and monitoring techniques of CO2 leakage from seafloor in sub-seabed CO2 storage. *Applied Geochemistry*, 30, 114-124.

Smolianski, A., H. Haario, and P. Luukka. 2008. “Numerical Study of Dynamics of Single Bubbles and Bubble Swarms.” *Applied Mathematical Modelling* 32 (5): 641–659. doi:10.1016/j.apm.2007.01.004.

Robbins, L.L., Hansen, M.E., Kleypas, J.A., and Meylan, S.C., 2010, CO2calc—A user-friendly seawater carbon calculator for Windows, Max OS X, and iOS (iPhone): U.S. Geological Survey Open-File Report 2010–1280, 17 p.

Wüest, A., N H Brooks, and D M Imboden. 1992. “Bubble Plume Modeling for Lake Restoration.” *Water Resources Research* 28 (12): 3235–3250.